NANOSYSTEMS:
PHYSICS, CHEMISTRY, MATHEMATICS

Ostroushko A.A., et al. *Nanosystems: Phys. Chem. Math.*, 2023, **14** (5), 571–583.
http://nanojournal.ifmo.ru
DOI 10.17586/2220-8054-2023-14-5-571-583

Original article

Synthesis of lanthanum manganite powders via combustion reactions: some aspects of the influence of magnetic field and charge generation in precursors on the formation of properties

Alexander A. Ostroushko, Iliya D. Gagarin, Egor V. Kudyukov, Tatiana Yu. Zhulanova, Anastasya E. Permyakova, Olga V. Russkikh

Ural Federal University Scientific Research Institute of Physics and Applied Mathematics, Ekaterinburg, Russia

Corresponding author: Alexander A. Ostroushko, alexander.ostroushko@urfu.ru

ABSTRACT The mutual influence of the process of electric charge generation in nitrate organic precursors and a constant external magnetic field on the magnetic properties formation was considered for lanthanum strontium manganite $La_{0.7}Sr_{0.3}MnO_{3\pm y}$ powders obtained via combustion reactions. The investigated properties of the obtained samples include hysteresis, magnetocaloric and magnetoresistive effects. The correlation between formation process of extended ensembles of nanoparticles and the functional properties of complex oxide materials was also discussed. The manifestation of a strong magneto-gas-selective effect has been observed during the combustion of precursors in a constant magnetic field, which affects the charge generation process.

KEYWORDS complex oxides, lanthanum manganite, synthesis, combustion reactions, nitrate-organic systems, nanoparticles, charges generation, magnetic properties, magneto-gas selective effect

ACKNOWLEDGEMENTS The research was financially supported by a grant from the Russian Science Foundation (Project No. 22-23-00718). The research was carried out using the equipment of the Ural Center for Collective Use “Modern Nanotechnologies”.

FOR CITATION Ostroushko A.A., Gagarin I.D., Kudyukov E.V., Zhulanova T.Yu., Permyakova A.E., Russkikh O.V. Synthesis of lanthanum manganite powders via combustion reactions: some aspects of the influence of magnetic field and charge generation in precursors on the formation of properties. *Nanosystems: Phys. Chem. Math.*, 2023, **14** (5), 571–583.

1. Introduction

Complex oxides based on lanthanum manganite with a perovskite-like structure are widely used as multifunctional materials, for example, in various sensor devices, energy converters and other due to their unique properties. They include magneto-optical properties [1], the presence of colossal magnetoresistance effects [2–5] and magnetocaloric properties [6–12] that are acceptable for practical, including biomedical, applications. In particular, the colossal magnetoresistance is due to the presence of manganese ions with oxidation states of $+3$ and $+4$ in the perovskite structure, leading to the emergence of kinetic ferromagnetic electron exchange and ferromagnetic ordering in doped manganites containing ions with mixed valences, which is achieved, for example, by introducing heterovalent substituents into the lanthanum sublattice. One of the most important aspects of the use of lanthanum manganite materials is their high catalytic properties [13–16]. Due to these properties, the aforementioned perovskites are used in solid oxide fuel cells and thermocatalytic devices for environmental protection. The functional properties of these materials are influenced by synthesis characteristics, particle size and morphology. In some cases, complex oxide materials consisting of nanoscale particles and their ensembles exhibit the most favorable properties. Methods based on the use of appropriate salts (often nitrates) as starting forms have significant advantages in the synthesis of such materials. Among the above-mentioned methods, Solution Combustion Synthesis (SCS) occupies one of the most important positions due to its simplicity of implementation, the possibility of varying the conditions for obtaining the materials, which makes it possible to control their properties. In particular, Solution Combustion Synthesis allows one to obtain highly efficient nanostructured complex oxide catalysts, including deposited ones [14, 17–19]. In addition, it is advisable to pay attention to the formation of magnetic properties of the materials during synthesis.

In addition to the target electromagnetic properties of lanthanum manganite-based perovskites, it is also important to consider the potential influence of the magnetic properties of catalytic materials on heterogeneous catalytic reactions [20–24], such as the combustion of toxic substances. The phenomenon of the so-called magnetogas-selective effect, which is based on the determinative flow of paramagnetic oxygen molecules from the air onto the catalyst surface and the expulsion of diamagnetic molecules of catalytic oxidation products and nitrogen, helps to increase the efficiency of thermocatalytic devices. At the same time, simultaneous reduction of nitrogen oxides occurs. Similar effects have been observed in liquid

reaction media. The magnetogas-selective effect could be used in various reactions to control their kinetics. On the surface of lanthanum manganite-based catalysts, heterogeneous redox reactions occur even at temperatures below 100 °C [14], where the catalytic material is able to exhibit ferromagnetic properties. Therefore, the possibility of the above effect should be considered.

The properties of complex oxide materials obtained via combustion reactions are influenced by such conditions as process temperature, composition and concentration of the gases formed. One of the important phenomena accompanying the synthesis processes of complex oxides by combustion of nitrate-organic precursors [5, 16, 19, 25–56] is the generation of high-density electric charges in the precursors and nanoparticles [45, 56–63]. The possibility of charge formation is associated with the release of ionized molecular groups into the gaseous environment and also with the lability of the oxidation state of transition metal ions which are the part of the precursors and the resulting material. The density of such charges correlates with the potential difference between the precursor and the earth, which can be conveniently measured [45], and its value reaches hundreds of volts. The potential differences detected on different sides of the combustion front during the implementation of the self-propagating high-temperature synthesis method do not exceed tenths or units of volts [64–71], and ionization of the gaseous environment is also possible when using this method. In many cases, the presence of charges during SCS determines the morphology of the synthesized complex oxides and has a significant impact on powder sintering processes. The temperature interval of intense sintering can be reduced by hundreds of degrees in the presence of high charges [57, 59]. The presence of high charges leads to mutual repulsion of nanoparticles, formation of small contact area between them, which significantly increases the reserve of excess surface energy of particles.

It should be noted that there is information in the literature on the influence of external magnetic fields on the formation of electromagnetic properties of complex oxides [72]. It seems interesting and useful to study how the combination of two factors – the presence of charges in the precursors and the influence of an external field – affects such properties. Previously [57], on the example of the lanthanum-strontium manganite $La_{0.7}Sr_{0.3}MnO_{3\pm y}$, it was found that the application of an external alternating electromagnetic field leads to a decrease in saturation magnetization and coercive force of the obtained materials, due to the disordering effect of the aforementioned field. The presence of medium intensity charge generation generally has a favorable effect on the hysteresis properties. The investigations in the above work [57] were carried out on samples with identical crystallographic structures and oxygen non-stoichiometry, which allows one to compare the results correctly. In this work we have investigated the influence of a constant magnetic field applied during synthesis on the magnetic properties of lanthanum-strontium manganites.

2. Experimental part

The synthesis of lanthanum manganite powders $LaMnO_{3\pm\delta}$, including doped $La_{0.7}Sr_{0.3}MnO_{3\pm\delta}$, was carried out by combustion of nitrate-organic precursors obtained by mixing two separately prepared solutions. The first one contained the respective metal nitrates dissolved in distilled water, the second one contained the organic component. Mixing the solutions resulted in the formation of precursors. The ratio of the organic part to the nitrates was stoichiometric ($\varphi = 1$) according to the combustion reaction [59] with the formation of water, carbon dioxide and nitrogen as the main gaseous products, or exceeded it ($\varphi > 1$). The following starting reagents (analytical grade) were used: lanthanum (III) nitrate hexahydrate $La(NO_3)_3 \cdot 6H_2O$, strontium nitrate $Sr(NO_3)_2$, manganese (II) nitrate tetrahydrate $Mn(NO_3)_2 \cdot 4H_2O$, glycine (Gly) NH_2CH_2COOH, polyvinyl alcohol (PVA) $(C_2H_4O)_n$ (viscosity of 4 % aqueous solution at room temperature 11 cP, content of residual acetate groups not exceeding 2 %) and polyvinyl pyrrolidone (PVP) $(C_6H_9NO)_n$ (molecular weight 40000, Sigma-Aldrich, PVP40).

For the preparation of precursors, two solutions were prepared separately in distilled water containing nitrates of the corresponding metals and an organic component. Solutions of polymer components (concentration of PVA or PVP – 5 or 10 wt.%, respectively) were prepared by heating in a water bath. When mixing the two solutions, the quantitative proportions were set in accordance with the stoichiometry of the nitrate combustion reaction with the formation of nitrogen, carbon dioxide and water as gaseous products [56]. The resulting solution was poured onto inert substrates, further evaporation of water (drying) took place at room temperature, this process took up to 7 days, as a result of which precursors in the form of films containing a stoichiometric amount of an organic component ($\varphi = 1$) or its double excess ($\varphi = 2$) were obtained. Combustion of precursors was carried out in porcelain cups using an alcohol lamp to initiate the combustion process. The combustion was carried out in the absence or under the influence of a constant magnetic field. The composition of gaseous combustion products (in particular, the concentration of nitrogen oxide NO, carbon monoxide CO) was determined using a Testo 350 XL gas analyzer (Testo, Germany). The final heat treatment was carried out at a temperature of 650 °C in the absence or under the influence of a constant magnetic field.

The synthesis was carried out after drying the precursor in air by placing it in a quartz tube reactor with an air flow of 2 l/min and heating it with an alcohol burner. The level of charge generation was determined as the potential difference between the precursor and the ground using an IPEP-1 electrostatic field meter (MNIPI, Republic of Belarus) with a special metal screen made of an inert material as the measuring lead. The device was calibrated by applying a potential of a given value to the screen using a B5-46 DC source (Priborelectro, Russian Federation). Similarly, to the method described above, synthesis was carried out by placing the reactor in a constant magnetic field created in the gap

between the electromagnet poles. Phase composition was determined by diffractometer D8 Advance (Bruker, Germany) in CuKa radiation ($\lambda = 1.5418$ Å). X-ray images were taken in the range of $20\ ^\circ \leq 2\theta \leq 80\ ^\circ$ with a step of 0.04 and a shutter speed of 1 second at the point. Phase identification was carried out using the Fpeak and MATCH! software packages. Alternatively, the pre-synthesized samples were annealed in a magnetic field. SEM was carried out by means of AURIGA CrossBeam scanning electron microscope (Carl Zeiss NTS, Germany); the data were controlled, monitored and analyzed using the Analysis Station software package, AURIGA series, version 3.7. The granulometric composition of the obtained powders was determined by laser diffraction on a SALD-7101 dispersion analyzer (Shimadzu, Japan). The hysteresis characteristics and magnetoresistance effect of the samples were measured using a LakeShore VSM 7407 (Lake Shore Cryotronics, USA) vibrating-sample magnetometer with the option of measuring magnetoresistance using compacted pressed samples. The magnetocaloric effect was measured by the direct method – the adiabatic temperature change was recorded when the magnetic field was switched on. The magnetic field was applied using a Halbach magnetic system; the field strength was up to 17 kOe. The system used allowed the field strength to change abruptly from 0 to maximum.

3. Results and discussion

Complex oxide samples $LaMnO_{3\pm\delta}$ and $La_{0.7}Sr_{0.3}MnO_{3\pm\delta}$ were synthesized by combustion of nitrate-organic precursors differing in organic component and its quantity. The combustion was carried out in the absence or under the influence of a constant magnetic field. Phase composition was controlled after the heat treatment at 650 °C. The XRD analysis showed that samples were single phase independently from the precursors' content and the conditions of both combustion and annealing. Lanthanum manganite $LaMnO_{3\pm\delta}$ and solid solutions on its base with R-3c spatial group were formed. The example of XRD patterns is shown in Fig. 1.

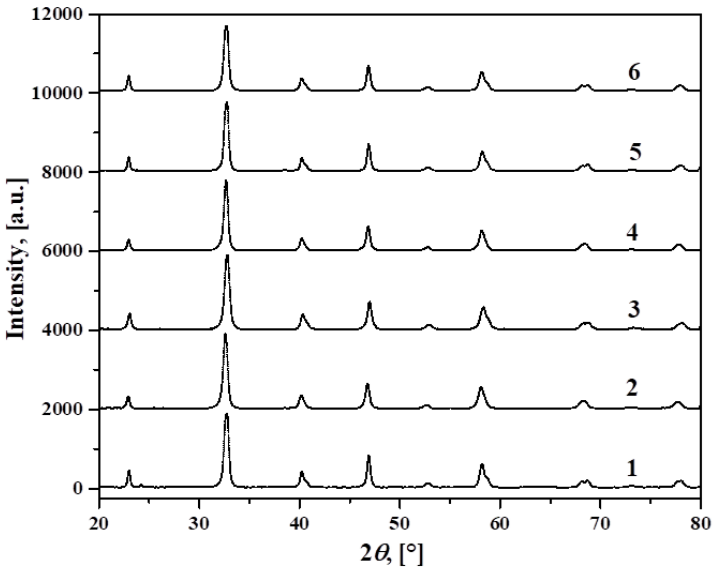

FIG. 1. XRD of $La_{0.7}Sr_{0.3}MnO_{3\pm\delta}$ samples synthesized from different precursors without impact of external magnetic field: 1 – PVP, $\varphi = 1$; 2 – PVP, $\varphi = 2$; 3 – PVA, $\varphi = 1$; 4 – PVA, $\varphi = 2$; 5 – Gly, $\varphi = 1$; 6 – Gly, $\varphi = 2$

Magnetic (hysteresis) characteristics of lanthanum strontium manganite samples synthesized under the influence of a constant magnetic field in the absence of a significant external electric field have been obtained (Fig. 2). An example of the experimental curves used to calculate the magnetic parameters is shown in Fig. 3. Experimental data (after two hours of annealing at 650 °C) revealed certain regularities in the formation of the magnetic properties of the samples, which can be roughly divided into three groups according to the intensity of the charge generation during the synthesis. The first group consists of samples whose synthesis was accompanied by high charge generation (potential difference ground – precursor was up to and above 100 V), the second one – samples with low intensity of charge generation (potential difference close to zero) and the last – samples in the average range for this parameter. The first group included materials synthesized from precursors containing PVA, the second – PVP and the third one – Gly. The first group of samples was characterized by the tendency to an increase of magnetic properties when a constant magnetic field was applied during the combustion of precursors. While for the samples from the second and third group the measured parameters decreased (coercive force, Curie temperature) or had a maximum at the average field strength (saturation magnetization) as the field strength applied during combustion increased.

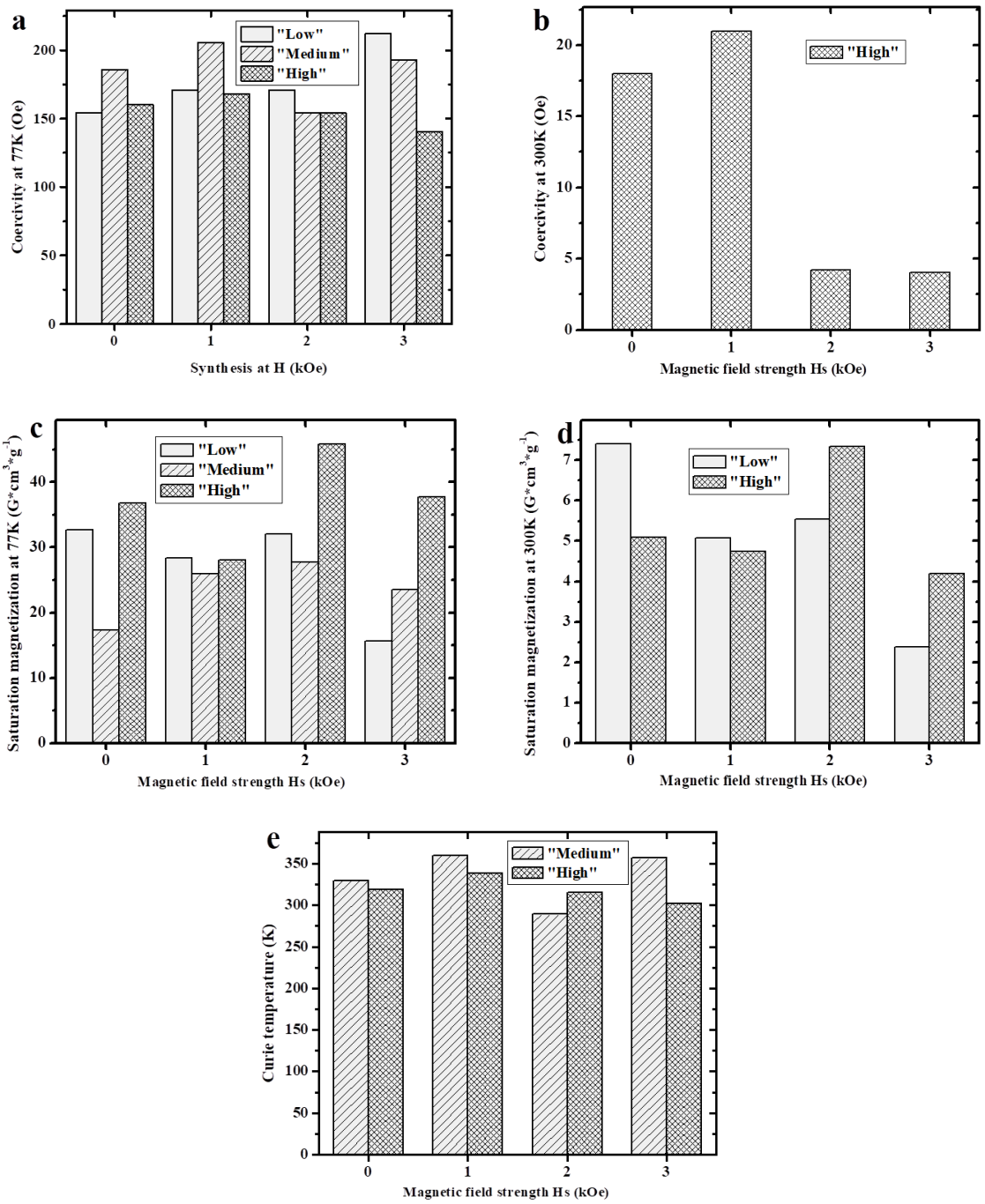

FIG. 2. Characteristics of the obtained samples. Hs is the strength of the magnetic field, which was applied during the synthesis

Analysis of the trends obtained from the experimental data shows that the saturation magnetization value also showed a maximum as a function of field strength (at 2 kOe) for the samples that had intermediate charges during synthesis. In contrast, the coercivity of the samples and the Curie temperature showed a minimum. Samples with low charges showed an increase in coercivity and Curie temperature with increasing field and the dependence with a maximum for magnetization. It should be noted that in this case the values of the magnetic parameters (saturation magnetization, Curie temperature) were higher for the samples obtained in the absence of an external field.

The maximum influence of the value of the external magnetic field strength applied during the synthesis on saturation magnetization value was observed for the samples with high generated charges, while the coercive force was more dependent on the change of the magnetic field for the samples with low values of generated charges. The maximum saturation magnetization values achieved in the described series of experiments had samples from the range of high generated charges, the coercive force values were higher for samples with medium and low charges. Correspondingly, the Curie

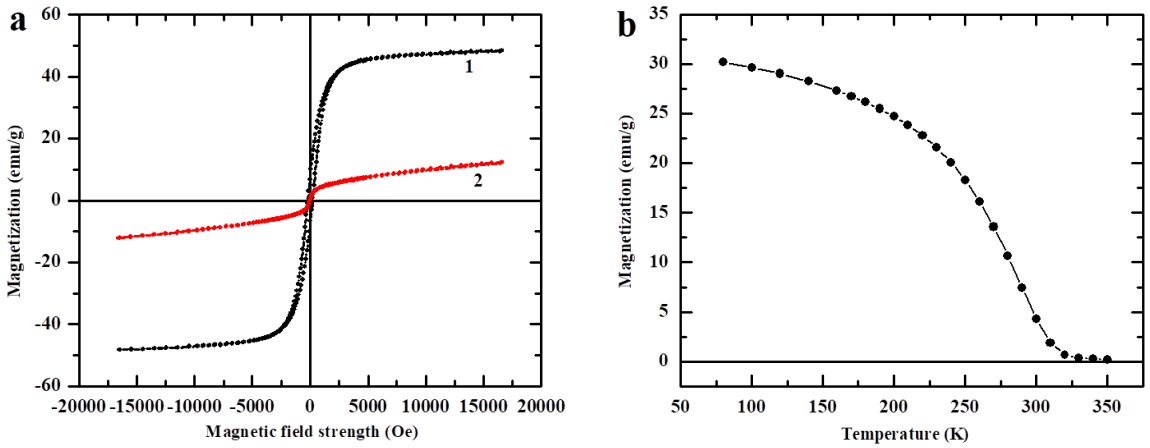

FIG. 3. Example of experimental magnetization dependence on (a) field strength for LSM sample (synthesized from PVA-containing precursor ($\varphi = 2$), combustion under the impact of external magnetic field 2Oe, annealed at 650 °C during 2 hours without impact of external magnetic field during thermal treatment): (1) black curve at 77 K; (2) red curve at 300 K; (b) temperature for LSM, obtained from PVA-containing precursor ($\varphi = 2$) annealed at 650 °C during 2 hours without impact of external magnetic field during combustion of precursor and thermal treatment

temperature was higher for samples with low charges. Based on the results obtained, it can be assumed that the presence of a magnetic field generally positively influences the formation of the magnetic structure of individual perovskite particles, which is most pronounced in the case of high charge generation in precursors during synthesis. However, the presence of high charges, as mentioned above, leads to strong mutual repulsion of nanoparticles and apparently prevents their specific aggregation into extended ensembles, which provides the increase of the coercive force, the Curie temperature. The dependence of the properties, e.g. the Curie temperature, on the effective size of the formations obtained in powders has already been noted [5, 73] for doped lanthanum manganites. There are also data on rather complicated correlations between the magnetic properties [5, 73] (magnetization) and the size and shape of manganite particles of different composition or their aggregates, which in turn may be related in particular to the magnetic moment of the manganese ions, the bonding angle of the Mn-O-Mn clusters in the nanoparticle structure, on their surface and at the interparticle boundaries. These aspects can also be influenced by synthesis conditions via combustion reactions (magnetic field effect, etc.), particle shape, packing density, etc.

Magnetocaloric and magnetoresistive effects were investigated for samples obtained under and without a magnetic field influence (for samples with different intensities of charge generation during the synthesis). Fig. 4 shows an example of the temperature dependence of the electrical resistivity measured in the absence of a magnetic field and in a constant magnetic field of 17 kOe or a compact sample of lanthanum strontium manganate in the form of a flat parallelepiped. The sample was obtained from a precursor containing a stoichiometric (for the combustion reaction) amount of glycine in a 3 kOe field. The coercive force was also higher for these samples (relatively low charges) (Fig. 2). The higher values compared to samples obtained from precursors with high charges may also indirectly indicate the positive effect of extended particle aggregation, which is not prevented by mutual repulsion of nanoparticles. Fig. 5 shows an example of the measurement of the magnetocaloric effect on a sample of doped lanthanum manganate characterized by the effect value of about 0.4 K in the temperature range $\sim$ 200 – 300 K. The sample was obtained from a precursor with intensive charge generation in the absence of an external field. For comparison, the result for the sample with bulk composition $La_{0.7}Ag_{0.3}MnO_{3\pm y}$ (synthesis in field 3 kOe, PVA $\varphi = 2$, low charges) is given. The indicated effects for the samples synthesized in combustion reactions have an acceptable value, which indicates the possibility of further studies to establish the influence of external electromagnetic fields during synthesis on the mentioned target parameters.

Regarding the formation of the morphology of the obtained samples, it could be noted that the possibility of obtaining a material containing extended ensembles of particles is associated with the superposition of at least two opposite factors. On the one hand, there is electrostatic repulsion between nanoparticles [74] due to charge generation, and on the other hand, magnetic interaction between particles is possible [75]. It can be assumed that an additional factor contributing to the minimization of particle contact is the presence of gases emitted during the combustion process. Considering the relatively low Curie temperature of the resulting samples, slightly above 100 °C, magnetic attraction with the emergence of the corresponding mutual spatial orientation is mainly possible below this temperature. In the absence of an external magnetic field, the residual (spontaneous) magnetization is the determining factor, while in the presence of a magnetic field it is induced by the field. In this case, we can assume that the formation of extended ensembles can occur mainly when the material cools down after the combustion of the precursor. In the literature, there are examples of modeling the

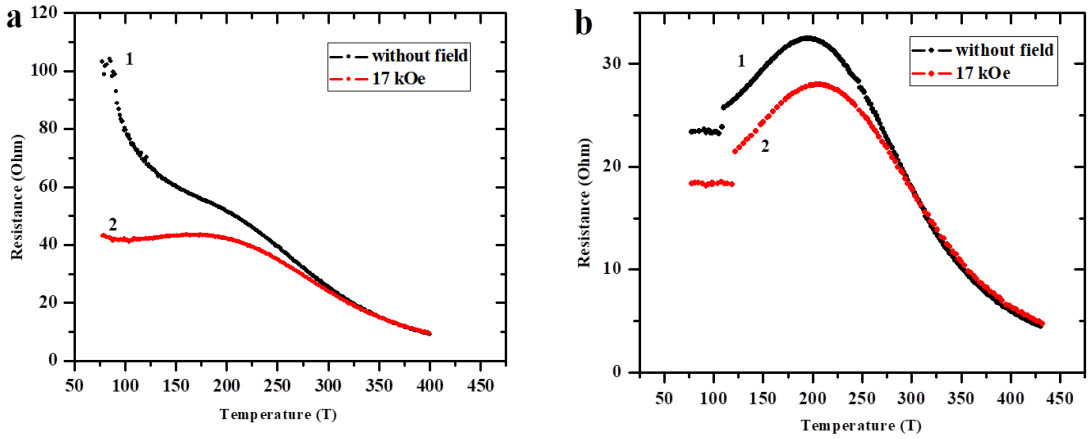

FIG. 4. Example of determining the magnetoresistance effect value: a – with a maximum value of 150 % at 77 K; 10 % at 0 °C and about 5 % at room temperature for lanthanum strontium manganate sample, synthesized from glycine containing precursor ($\varphi = 1$) in a field of 3 kOe; b – lanthanum strontium manganate sample, synthesized from glycine containing precursor ($\varphi = 2$) in a field of 3 kOe

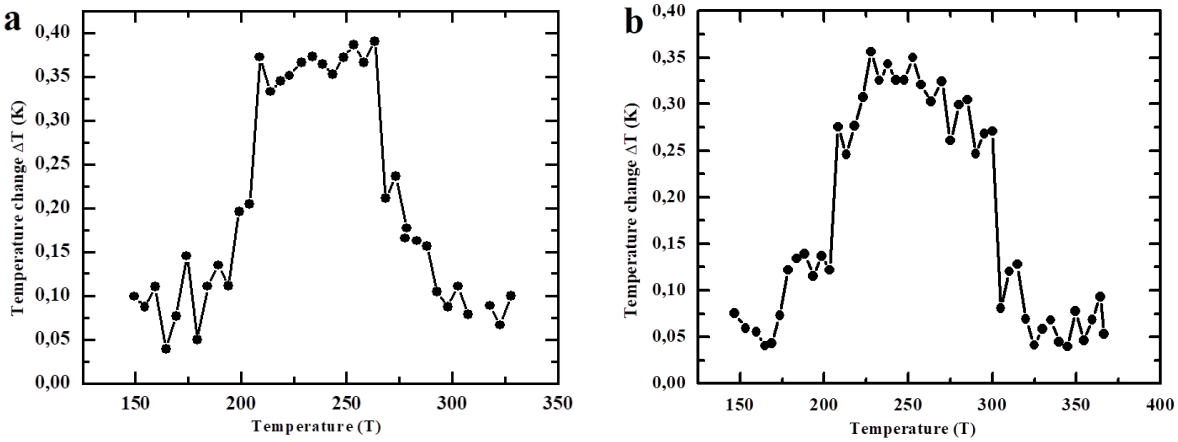

FIG. 5. Examples of magnetocaloric effect measurements for samples: a – $La_{0.7}Sr_{0.3}MnO_{3\pm y}$; b – $La_{0.7}Ag_{0.3}MnO_{3\pm y}$

superposition of attraction and repulsion forces [76] (the interaction potential V), in particular, during the formation of extended structures of ferrogels in a liquid medium [74, 77–79], using the corresponding equations. When considering the interaction potential V of the particles formed in combustion reactions, in principle, the closely acting van der Waals forces [80] can also be taken into account. However, these forces do not contribute significantly (Fig. 6). In contrast to the particles of gels, steric repulsion, which is typical for colloidal systems, is not taken into account [81]. The relatively low permittivity of the gas medium compared to aqueous solutions, where ferrogels and similar formations are formed, should be considered. This will weaken the electrostatic repulsion.

An approximate scheme of the interaction potential V of manganite particles may look as follows (Fig. 6). Such a consideration approximates the interaction of at least two complex oxide particles at the initial stage of their chain formation. In this case, the real sizes of the particles and the effective distances between them in the $La_{0.7}Sr_{0.3}MnO_{3\pm y}$ sample can be used to estimate the above potentials (Fig. 7). If the average size of a "cell" occupied by each particle is assumed to be 100 nm, then according to [61], where the charge density on the precursor surface is given as $\sim 2 \cdot 10^{-6}$ C/cm^2 or 10^{13} elementary charges per 1 cm^2, we can estimate the charge of each of the 10^{10} particles to be of the order of $2 \cdot 10^{-16}$ C. This corresponds to the order of 10^3 excess charges per particle or evaluated by 1 excess elementary charge per $3.5 \cdot 10^5$ crystallographic cells of lanthanum-strontium-manganite. The potential of electrostatic repulsion between particles by means of Coulomb's law in such a case is evaluated as 18 V, which corresponds to rather typical measured potential difference ground – precursor in the process of synthesis of complex oxides. This value increases with higher charge densities and correspondingly higher precursor-ground potential difference U.

Consideration of the estimated resultant curve for electrostatic repulsion and magnetic interaction of particles (Fig. 6) at different precursor charges indicates the possibility of self-organization and formation of extended magnetic formations in the region of intermediate charges. Despite the approximate nature of the estimation, a correlation with the actually

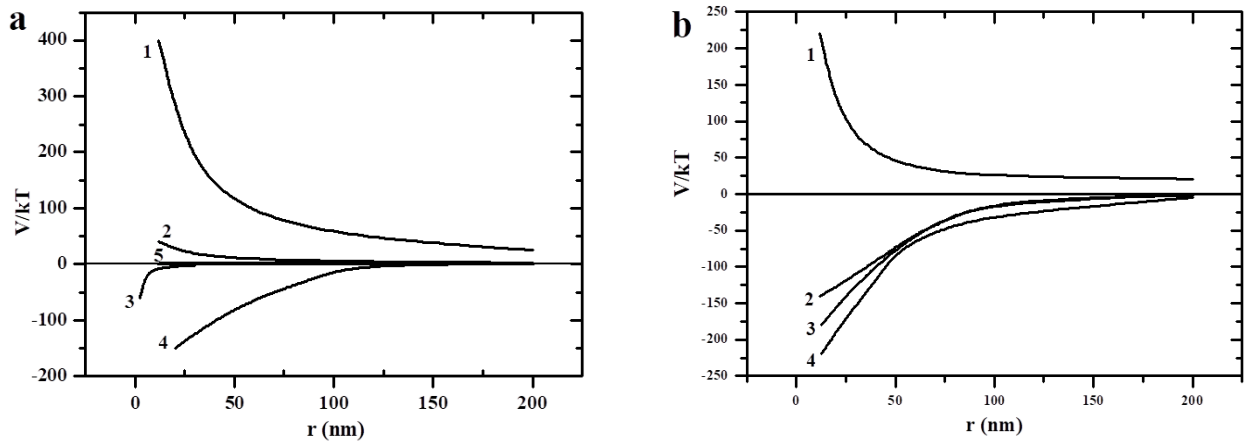

FIG. 6. The dependence of interaction potential of particles V/kT from the distance between particles: a – electrostatic repulsion at a potential difference ground – precursor 1, 10, 100 V (bottom-up), van der Waals force and magnetic interaction; b – resultant curves for the same potential difference ground – precursor

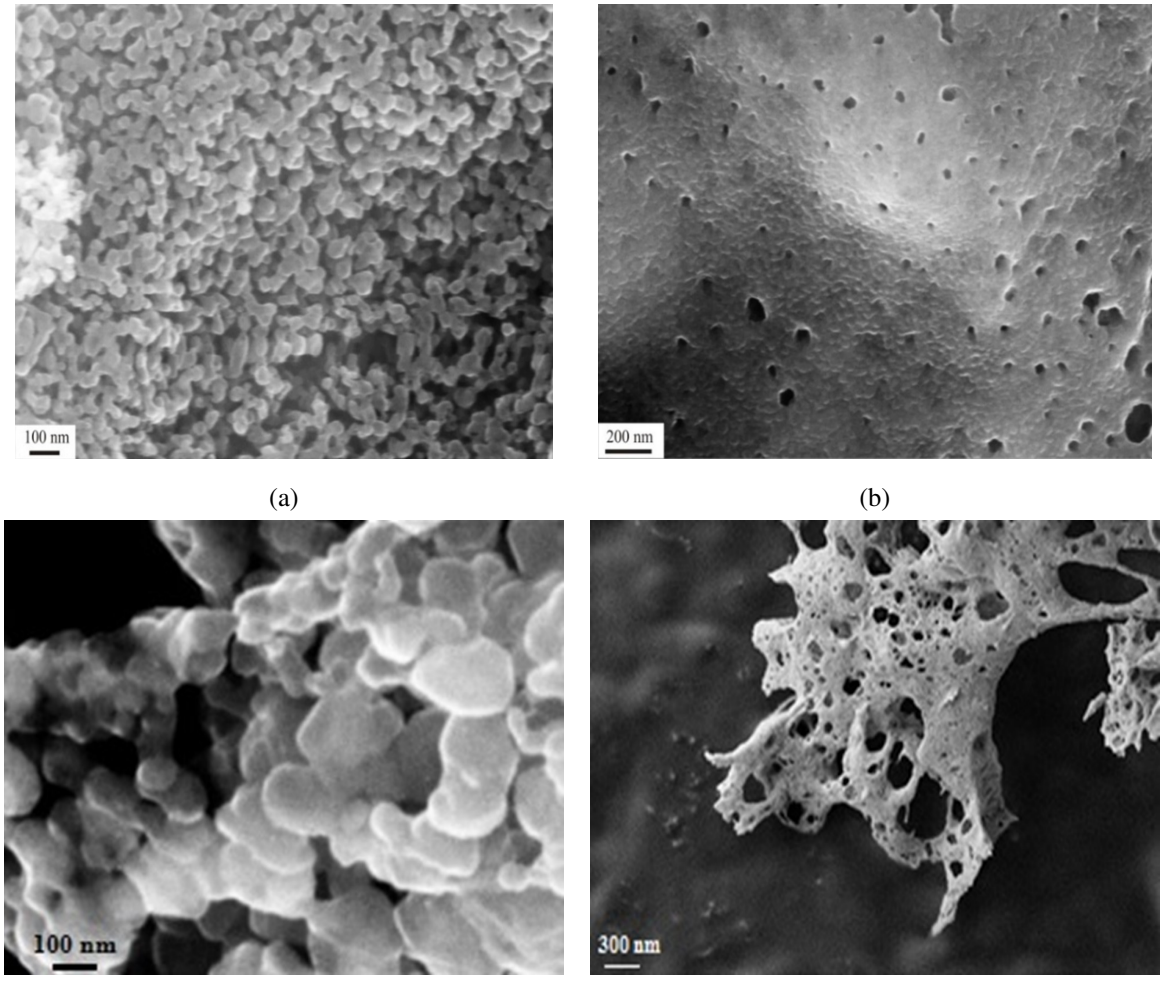

FIG. 7. SEM of $La_{0.7}Sr_{0.3}MnO_{3\pm y}$ samples, obtained by combustion of PVA containing precursors with different φ value: a – potential difference ground – precursor fixed during synthesis about 200 V (weak particle contact); b – potential difference ground – precursor fixed during synthesis about 10 – 20 V (dense contact); c – beginning of chain aggregates formation; d – fractal (branched structures). SEM images were obtained without changing the integrity of the fragments of materials synthesized via combustion reactions

observed interparticle interactions can be seen. Thus, the generation of high charges leads to the predominance of repulsive forces, while relatively low charges or their practical absence lead to denser contacts between particles (Fig. 7). It is noteworthy that the particles themselves are close in size, which is apparently determined by physicochemical features of the oxide material synthesis processes under combustion reaction conditions [82, 83]. Resulting particles with a size of 50 – 350 nm form submicron and micron aggregates up to 20 μm (Fig. 7). Certain regularity can be observed in the spatial arrangement of the particles. The difference in powders obtained from precursors with different charge generation intensities is clearly seen when comparing their intense sintering temperature [57, 59]. This difference is also clearly seen in the dependence of the specific surface area on the value of the generated potential difference ground – precursor (Fig. 8). It is very interesting that for deterministic [82, 83] particle sizes of complex oxides of different compositions, the dependence of the specific surface area of powders on the above potential difference is practically the same. This can be seen, for example, for doped lanthanum manganite and cerium iron oxide (Fig. 9).

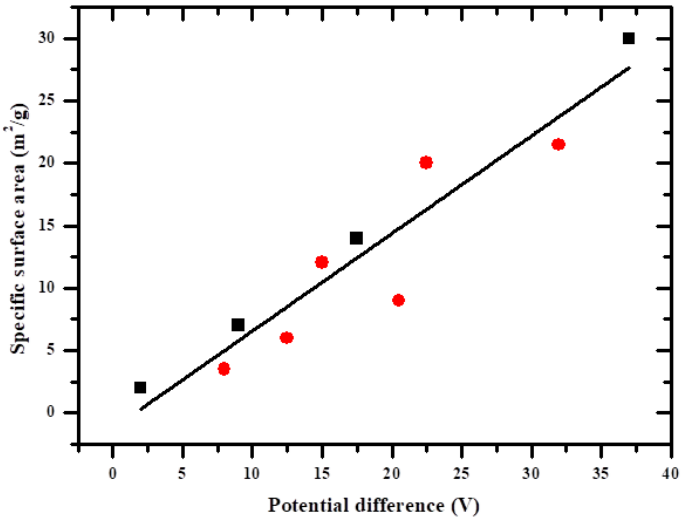

FIG. 8. The dependence of the specific surface area (m^2/g) on the maximum potential difference (V) of the precursor-ground during synthesis from organic nitrate compositions of complex oxides $Ce_{0.9}Fe_{0.1}O_2$ [65] (circles) and lanthanum manganites (squares)

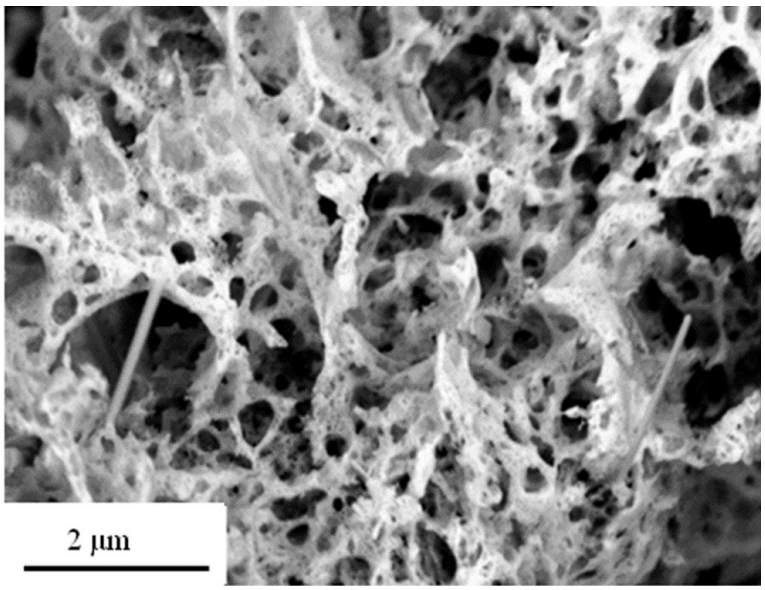

FIG. 9. SEM of $Ce_{0.9}Cu_{0.1}O_2$ sample synthesized from PVA containing precursor ($\varphi = 1$)

Apparently, the chains of nanoparticles are not limited to their ability to associate by magnetic interaction. If such particles have more than two active interaction centers, the chains can branch into Y and X (Fig. 7) and more complex chains with the formation of dendritic (fractal) structures, the mechanism of whose formation is described in the literature,

at least for such objects as magnetic fluids [84]. It can be assumed that in the future it would be productive to use a mathematical technique similar to the models of such media as magnetic fluids and ferrogels to describe and predict the behavior of systems in which the synthesis of magnetic nanoparticles takes place. It is clear that our approach to estimating the possibility of forming extended ensembles of nanoparticles is quite suitable for the systems in which complex oxides exhibit ferromagnetic properties at much higher temperatures than lanthanum manganites. In the first place it concerns hexaferrites Sr, Ba with magnetoplumbite-type structure, since the Curie temperature of such complex oxides is equal to their synthesis temperature in combustion reactions. It should also be assumed that the resulting curve of interaction potentials between particles V for complex oxides, including lanthanum manganite, under the influence of magnetic field, at the same intensity of charge generation U, will be located below the curve obtained in the absence of external field (Fig. 6). It is clear that exposure to an external magnetic field, other conditions being equal, increases the tendency to form nanoparticle chain associations by increasing the magnetization of the material. At the same time, dendritic associates similar to those observed for manganites (Fig. 7) can also be found in other systems whose morphology formation is not related to magnetic interaction. A sample based on cerium dioxide (Fig. 9) can serve as an example. It can be assumed that one of the conditions determining the formation of dendritic structures is usually an intensive volumetric combustion of the precursor. On the other hand, proper chain ensembles are most likely to be formed under smoldering combustion or close to the SHS regime.

Some additional assumptions about the processes of synthesis of complex oxide materials via combustion of organic nitrate precursors could be proposed. Some peculiarities of obtaining the double perovskite $Sr_2Ni_{0.7}Mg_{0.3}MoO_{6-d}$ [60] as a potential anode material for solid oxide fuel cells have already been considered. This and similar materials exhibit ferromagnetic properties only at rather low temperatures due to the low Curie temperature [83, 85]. However, the formation of the target product occurs through the appearance of intermediate oxide products containing either molybdenum or nickel. At the same time, the formation of nano-sized molybdenum oxide particles with an intermediate degree of oxidation, which can form in the presence of organic compounds, nickel oxide and other phases, which may also have magnetic properties and give rise to extended ensembles, as observed in electron micrographs of samples [60], cannot be excluded. The presence of such chains may also contribute to the high electrical conductivity of the material [60], obtained from a precursor with sufficiently intense charge generation. Another important point is the possibility of generating charges of different sign on the particles of the intermediate phases, which differ in the presence of transition metal ions (Ni, Mo). The sign of the charge, among other conditions, is related to the tendency of such ions to change the direction of the degree of oxidation [57]. In case of formation of charges of different signs, such nanoparticles will experience a sufficiently strong mutual attraction, judging by the value of the electrostatic interaction potentials discussed above. This point will probably contribute to a good contacting of the intermediate phase particles and facilitate the synthesis of the final product, as observed in [60].

Further research can include aspects such as the formation of extended structures in complex oxide materials during their synthesis when coatings are deposited on substrates using combustion reactions. In such a case, the texturing factors are the electrostatic repulsion of the particles and the topological orientation effect of the substrate. An example is the textured coating of $YBa_2Cu_3O_{7-\delta}$ on an oxide support (Fig. 10); in precursors based on the respective metal nitrates and polyvinyl alcohol, the appearance of charges of negative sign was recorded [61].

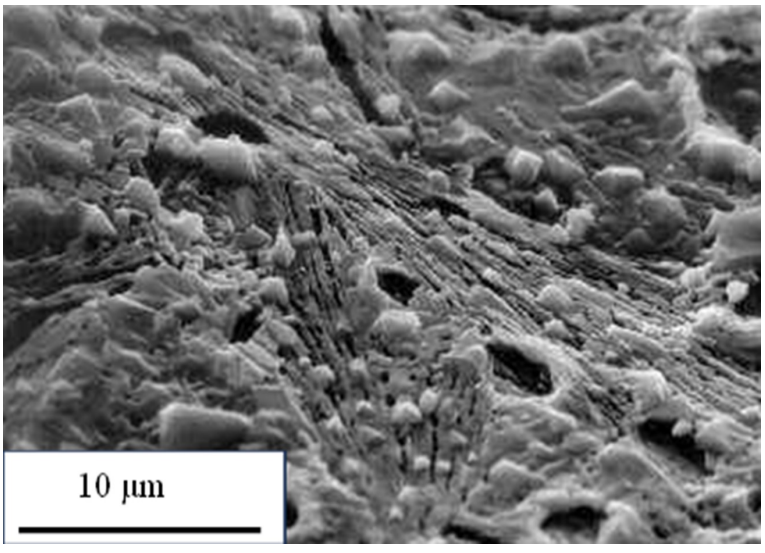

FIG. 10. SEM of $YBa_2Cu_3O_{7-\delta}$ coating on an Al_2O_3 carrier with a zirconium dioxide sublayer obtained by pyrolysis of nitrate-polyvinyl alcohol compositions [86]

Another important point concerning the synthesis processes discovered during the study should be noted. A fairly strong manifestation of the magnetic-gas-selective effect during the combustion of organo-nitrate compositions was established. This effect was discussed above [20–24]. In this case, during the precursor (PVA, $\varphi = 1$) combustion in a magnetic field ($H = 3$ kOe), the potential difference U of the order of $+60$ V was determined while this value was about -8 V when the combustion of the same precursor occurred in the absence of a magnetic field. It should be noted that the value of U reached $+100$ V and even more when the combustion occurs under the influence of an electromagnetic field [59]. Consequently, a constant magnetic field prevented the removal of negatively charged paramagnetic molecular groups like H_2O^-, CO_3^- during combustion, whereas the application of an alternating electromagnetic field, on the contrary, promoted it [50, 59]. The pattern established initially allows us to control the process of charge generation and influence the formation of the morphology of the samples; it requires further study. On the other hand, this point makes more understandable the results of formation of magnetic properties of samples (Fig. 2), where non-monotone dependence on the external field strength is observed, because the intensity of manifestation of the magnetic-gas-selective effect may be related to the field strength.

4. Conclusion

In conclusion, it should be noted that the influence of the magnetic field on the results of synthesis of lanthanum manganites appears in a rather complex superposition with such a factor as the presence and intensity of generation of electric charges, determined by synthesis conditions, in particular, the composition of precursors. Nevertheless, it is possible to trace the regularity of such mutual influence. When considering the effect of magnetic field, it is reasonable to divide the studied systems into groups according to the intensity of charge generation: high, medium and low. An external magnetic field had a predominantly positive influence on the lanthanum-strontium-manganite samples, in which high intensity of charge generation was observed in terms of their magnetization enhancement, apparently due to obtaining a more perfect magnetic structure of crystallites. Under conditions of medium and low intensity of charge generation, when the electrostatic repulsive forces are lower, but still strong enough to minimize contacts between nanoparticles, conditions are created for the formation of chain-like ensembles as well as dendritic forms. At the same time, the application of a magnetic field has a positive effect on the value of the coercive force of the samples, and increase of the Curie temperature. The use of the detected trends allows one to purposefully optimize the conditions of manganite production, including the choice of the conditions for obtaining materials with such properties as magnetocaloric and magnetoresistance effects, on the basis of the available data on the intensity of charge generation in a given system of starting reagents. A magneto-gas-selective effect was found to occur during the combustion of nitrate organic precursors, leading to a decrease in the resulting potential difference between the ground and the precursor. This phenomenon requires further detailed investigation.

References

[1] Sukhorukov Yu. P., Gan'shina E.A., Loshkareva N.N., Kaul A.R., Gorbenko O.Yu., Telegin A.V., et al. Evolution of magnetooptical and transport properties of $La_{1-x}Ag_xMnO_3$ films depending on silver concentration. *J. Exp. Theor. Phys.*, 2007, **104** (4), P. 569–576.

[2] Vasil'ev A.V., Vizgalov V.A., Trusov L.A., Kazin P.E., Tret'yakov Yu.D., Jansen M. Magnetoresistive composites $La_{0.7}Sr_{0.3}MnO_{3-\delta}$ – PMMA. *Dokl. Chem.*, 2012, **445** (1), P. 137–139.

[3] Kaul A.R., Gorbenko O.Y., Kamenev A.A. The role of heteroepitaxy in the development of new thin-film oxide-based functional materials. *Russ. Chem. Rev.*, 2004, **73** (9), P. 861–880.

[4] Gamzatov A.G., Batdalov A.B., Melnikov O.V., Gorbenko O.Yu. Spin-polarized transport in the manganite $La_{0.85}Ag_{0.15}MnO_3$. *Low Temp. Phys.*, 2009, **35** (3), P. 219–222.

[5] Teplykh A.E., Bogdanov S.G., Valiev É.Z., Pirogov A.N., Dorofeev Yu.A., Ostroushko A.A., et al. Size effect in nanocrystalline manganites $La_{1-x}A_xMnO_3$ (A=Ag, Sr). *Phys. Solid State*, 2003, **45** (12), P. 2328–2333.

[6] Bubnovskaya L., Belous A., Solopan S., Kovelskaya A., Bovkun L., Podoltsev A., et al. Magnetic Fluid Hyperthermia of Rodent Tumors Using Manganese Perovskite Nanoparticles. *J. of Nanoparticles*, 2014, **2014**, P. 1–9.

[7] Zheng L., Chen Y., Wang Y., Wang P., Wang T. Effect of Bi Ions on the Hyperthermia Properties of Hyaluronic Acid-Coated $La_{1-x}Sr_xMnO_3$ Nanoparticles. *NANO*, 2020, **15** (01), 2050015.

[8] Wu S., Wang Y., Shi D. Positively Charged Magnetic Nanoparticles for Capture of Circulating Tumor Cells from Clinical Blood Samples. *Nano LIFE*, 2020, **10** (03), 1971001.

[9] Estemirova S.K., Mitrofanov V.Y., Uporov S.A., Kozhina G.A. Magnetocaloric properties of Fe-substituted La–Sr-manganites. *Solid State Sciences*, 2022, **124**, 106806.

[10] Szewczyk A., Gutowska M., Piotrowski K., Dabrowski B. Direct and specific heat study of magnetocaloric effect in $La_{0.845}Sr_{0.155}MnO_3$. *J. Appl. Phys.*, 2003, **94** (3), P. 1873–1876.

[11] Gamzatov A.G., Aliev A.M., Batdalov A.B., Abdulvagidov Sh.B., Mel'nikov O.V., Gorbenko O.Yu. Magnetocaloric effect in silver-doped lanthanum manganites. *Tech. Phys. Lett.*, 2006, **32** (6), P. 471–473.

[12] Gamzatov A.G., Khizriev K.Sh., Batdalov A.B., Abdulvagidov Sh.B., Aliev A.M., Melnikov O.V., et al. Critical behavior of the specific heat of manganites $La_{1-x}Ag_xMnO_3$ ($x = 0.1, 0.15, 0.2$) near the Curie point. *Low Temp. Phys.*, 2009, **35** (3), P. 214–218.

[13] Ifrah S., Kaddouri A., Gelin P., Leonard D. Conventional hydrothermal process versus microwave-assisted hydrothermal synthesis of $La_{1-x}Ag_xMnO_{3+\delta}$ ($x = 0, 0.2$) perovskites used in methane combustion. *Comptes Rendus Chimie*, 2007, **10** (12), P. 1216–1226.

[14] Ostroushko A.A., Shubert E., Makarov A.M., Minyaev V.I., Udilov A.E., Elokhina L.V., et al. Catalytic Activity of Complex-Oxide Perovskite-containing Compositions in Reactions of Oxidation of CO and Organic Compounds. *Russ. J. Appl. Chem.*, 2003, **76** (8), P. 1253–1259.

[15] Kalinina E.G., Pikalova E.Yu. New trends in the development of electrophoretic deposition method in the solid oxide fuel cell technology: theoretical approaches, experimental solutions and development prospects. *Russ. Chem. Rev.*, 2019, **88** (12), P. 1179–1219.

[16] Russkikh O.V., Ivanov D.V., Isupova L.A., Chezganov D.S., Ostroushko A.A. Synthesis, morphology, and activity of $La_{1-x}Ag_xMnO_{3\pm y}$ catalysts. *Kinet. Catal.*, 2016, **57** (5), P. 712–721.

[17] Ostroushko A.A., Russkikh O.V., Kormil'tzev I.I., Kolosov V.Yu., Tsvetkov D.S., Vylkov A.I. Study of nanostructured catalysts on the basis of complex oxides deposited on a carrier. *J. Synch. Investig.*, 2011, **5** (4), P. 677–682.

[18] Ostroushko A.A., Russkikh O.V. Catalytic properties of complex oxide coatings on foamed nickel. *Russ. J. Appl. Chem.*, 2015, **88** (10), P. 1582–1588.

[19] Ostroushko A.A., Russkikh O.V., Chezganov D.S. Formation and morphology of nickel foam–complex oxide coatings with the perovskite structure. *J. Synch. Investig.*, 2015, **9** (6), P. 1237–1242.

[20] Yao G., Wang F., Wang X., Gui K. Magnetic field effects on selective catalytic reduction of NO by NH_3 over Fe_2O_3 catalyst in a magnetically fluidized bed. *Energy*, 2010, **35** (5), P. 2295–2300.

[21] Wang D., Pan J., Zhu D., Guo Z., Yang C., Duan X. Enhanced adsorption of NO onto activated carbon by gas pre-magnetization. *Sci. Total Environ.*, 2022, **830**, 154712.

[22] Xie Y., Wang M., Wang X., Wang L., Ning P., Ma Y., et al. Magnetic-field-assisted catalytic oxidation of arsine over Fe/HZSM-5 catalyst: Synergistic effect of Fe species and activated surface oxygen. *J. Clean. Prod.*, 2022, **337**, 130549.

[23] Nikitin V.A. *Lekzii po teplotekhnike*. Orenburg State University, Orenburg, 2011, 532 p.

[24] Cai Y., Zou H., Qu G., Li J., Che L., Hu Y., et al. The mechanism of catalytic oxidation phosphine in liquid phase by transition metal magnetic catalyst in external magnetic field. *Environ. Technol. Innov.*, 2022, **28**, 102958.

[25] Xu C., Manukyan K.V., Adams R.A., Pol V.G., Chen P., Varma A. One-step solution combustion synthesis of CuO/Cu_2O/C anode for long cycle life Li-ion batteries. *Carbon*, 2019, **142**, P. 51–59.

[26] Pikalova E., Kolchugin A., Zakharchuk K., Boiba D., Tsvinkinberg V., Filonova E., et al. Mixed ionic-electronic conductivity, phase stability and electrochemical activity of Gd-substituted $La_2NiO_{4+\delta}$ as oxygen electrode material for solid oxide fuel/electrolysis cells. *Int. J. Hydrog.*, 2021, **46** (32), P. 16932–16946.

[27] Khaliullin Sh.M., Koshkina A.A. Influence of fuel on phase formation, morphology, electric and dielectric properties of iron oxides obtained by SCS method. *Ceram. Int.*, 2021, **47** (9), P. 11942–11950.

[28] Popkov V.I., Almjasheva O.V., Nevedomskiy V.N., Panchuk V.V., Semenov V.G., Gusarov V.V. Effect of spatial constraints on the phase evolution of $YFeO_3$-based nanopowders under heat treatment of glycine-nitrate combustion products. *Ceram. Int.*, 2018, **44** (17), P. 20906–20912.

[29] Tugova E., Yastrebov S., Karpov O., Smith R. $NdFeO_3$ nanocrystals under glycine nitrate combustion formation. *J. Cryst. Growth*, 2017, **467**, P. 88–92.

[30] Wang X., Qin M., Fang F., Jia B., Wu H., Qu X., et al. Effect of glycine on one-step solution combustion synthesis of magnetite nanoparticles. *J. Alloys Compd.*, 2017, **719**, P. 288–295.

[31] Lomanova N.A., Tomkovich M.V., Osipov A.V., Ugolkov V.L., Danilovich D.P., Panchuk V.V., et al. Formation of $Bi_{1-x}Ca_xFeO_{3-\delta}$ Nanocrystals via Glycine-Nitrate Combustion. *Russ. J. Gen. Chem.*, 2019, **89** (9), P. 1843–1850.

[32] Popkov V.I., Almjasheva O.V., Semenova A.S., Kellerman D.G., Nevedomskiy V.N., Gusarov V.V. Magnetic properties of $YFeO_3$ nanocrystals obtained by different soft-chemical methods. *J. Mater. Sci. Mater. Electron.*, 2017, **28** (10), P. 7163–7170.

[33] Lomanova N.A., Tomkovich M.V., Sokolov V.V., Gusarov V.V. Special features of formation of nanocrystalline $BiFeO_3$ via the glycine-nitrate combustion method. *Russ. J. Gen. Chem.*, 2016, **86** (10), P. 2256–2262.

[34] Popkov V.I., Almjasheva O.V. Yttrium orthoferrite YFeO3 nanopowders formation under glycine-nitrate combustion conditions. *Russ. J. Appl. Chem.*, 2014, **87** (2), P. 167–171.

[35] Lomanova N.A., Tomkovich M.V., Sokolov V.V., Ugolkov V.L., Panchuk V.V., Semenov V.G., et al. Thermal and magnetic behavior of $BiFeO_3$ nanoparticles prepared by glycine-nitrate combustion. *J. Nanopart. Res.*, 2018, **20** (2), 17.

[36] Ostroushko A.A., Shubert E., Zhuravleva L.I. Synthesis and physicochemical and catalytic properties of perovskites $ABO_{3\pm y}$ (A = La, Sr, Ag; B = Mn, Co, Fe, Cu, Ti, Mo, V). *Russ. J. Appl. Chem.*, 2000, **73** (8), 1311.

[37] Zaboeva E.A., Izotova S.G., Popkov V.I. Glycine-nitrate combustion synthesis of $CeFeO_3$-based nanocrystalline powders. *Russ. J. Appl. Chem.*, 2016, **89** (8), P. 1228–1236.

[38] Farhadi S., Zaidi M. Bismuth ferrite ($BiFeO_3$) nanopowder prepared by sucrose-assisted combustion method: A novel and reusable heterogeneous catalyst for acetylation of amines, alcohols and phenols under solvent-free conditions. *J. Mol. Catal. A: Chem.*, 2009, **299** (1–2), P. 18–25.

[39] Farbun I.A., Romanova I.V., Khainakov S.A., Kirillov S.A. Properties of nanosized materials on the base of manganese and cerium oxides obtained from the citric solutions. *Surface*, 2010, **2** (17), 197.

[40] Delimaris D., Ioannides T. VOC oxidation over MnOx–CeO_2 catalysts prepared by a combustion method. *Appl. Catal. B*, 2008, **84** (1–2), P. 303–312.

[41] Delimaris D., Ioannides T. VOC oxidation over CuO–CeO_2 catalysts prepared by a combustion method. *Appl. Catal. B*, 2009, **89** (1–2), P. 295–302.

[42] Rao G.R., Sahu H.R., Mishra B.G. Surface and catalytic properties of Cu–Ce–O composite oxides prepared by combustion method. *Colloids Surf. A Physicochem. Eng. Asp.*, 2003, **220** (1–3), P. 261–269.

[43] Mahour L.N., Choudhary H.K., Kumar R., Anupama A.V., Sahoo B. Structural, optical and Mössbauer spectroscopic investigations on the environment of Fe in Fe-doped ZnO ($Zn_{1-x}Fe_xO$) ceramics synthesized by solution combustion method. *Ceram. Int.*, 2019, **45** (18), P. 24625–24634.

[44] Komlev A.A., Gusarov V.V. Glycine-nitrate combustion synthesis of nonstoichiometric Mg–Fe spinel nanopowders. *Inorg. Mater.*, 2014, **50** (12), P. 1247–1251.

[45] Ostroushko A.A., Russkikh O.V., Gagarin I.D., Filonova E.A. Study of the charge generation in the synthesis of nanosized complex oxides in the combustion reactions of organo-inorganic precursors. *Phys. Chem. Aspect. Stud. Clust. Nanostr. Nanomater.*, 2019, **11**, 215.

[46] Chick L.A., Pederson L.R., Maupin G.D., Bates J.L., Thomas L.E., Exarhos G.J. Glycine-nitrate combustion synthesis of oxide ceramic powders. *Mater. Lett.*, 1990, **10** (1–2), P. 6–12.

[47] Popkov V.I., Almjasheva O.V., Nevedomskiy V.N., Sokolov V.V., Gusarov V.V. Crystallization behavior and morphological features of $YFeO_3$ nanocrystallites obtained by glycine-nitrate combustion. *Nanosystems: Phys. Chem. Math.*, 2015, **6** (6), P. 866–874.

[48] Chiu T.-W., Yu B.-S., Wang Y.-R., Chen K.-T., Lin Y.-T. Synthesis of nanosized $CuCrO_2$ porous powders via a self-combustion glycine nitrate process. *J. Alloys Compd.*, 2011, **509** (6), P. 2933–2935.

[49] Enikeeva M.O., Kenges K.M., Proskurina O.V., Danilovich D.P., Gusarov V.V. Influence of Hydrothermal Treatment Conditions on the Formation of Lanthanum Orthophosphate Nanoparticles of Monazite Structure. *Russ. J. Appl. Chem.*, 2020, **93** (4), P. 540–548.

[50] Khaliullin Sh.M., Bamburov V.G., Russkikh O.V., Ostroushko A.A., Zhuravlev V.D. $CaZrO_3$ synthesis in combustion reactions with glycine. *Dokl. Chem.*, 2015, **461** (2), P. 93–95.

[51] Smirnova M.N., Goeva L.V., Simonenko N.P., Beresnev E.N., Kop'eva M.A., Ketsko V.A. Gel formation specifics in the synthesis of $Mg(Fe_{0.8}Ga_{0.2})_2O_4$ by the glycine–nitrate method. *Russ. J. Inorg. Chem.*, 2016, **61** (10), P. 1301–1306.

[52] Zhuravlev V.D., Bamburov V.G., Beketov A.R., Perelyaeva L.A., Baklanova I.V., Sivtsova O.V., et al. Solution combustion synthesis of α-Al_2O_3 using urea. *Ceram. Int.*, 2013, **39** (2), P. 1379–1384.
[53] Khaliullin Sh.M., Zhuravlev V.D., Bamburov V.G. Solution-combustion synthesis of oxide nanoparticles from nitrate solutions containing glycine and urea: Thermodynamic aspects. I*nt. J. Self-Propag. High-Temp. Synth.*, 2016, **25** (3), P. 139–148.
[54] Ostroushko A.A., Mogil'nikov Y.V., Ostroushko I.P. Synthesis of Molybdenum-and Vanadium-Containing Mixed Oxides in Polymer-Salt Systems. *Inorg. Mater.*, 2000, **36** (12), P. 1256–1263.
[55] Popkov V.I., Almjasheva O.V., Schmidt M.P., Izotova S.G., Gusarov V.V. Features of nanosized $YFeO_3$ formation under heat treatment of glycine–nitrate combustion products. *Russ. J. Inorg. Chem.*, 2015, **60** (10), P. 1193–1198.
[56] Ostroushko A.A., Russkikh O.V. Oxide material synthesis by combustion of organic-inorganic compositions. *Nanosystems: Phys. Chem. Math.*, 2017, **8** (4), P. 476–502.
[57] Ostroushko A.A., Maksimchuk T.Yu., Permyakova A.E., Russkikh O.V. Determinative Factors for the Thermochemical Generation of Electric Charges upon Combustion of Nitrate–Organic Precursors for Materials Based on Lanthanum Manganite and Cerium Dioxide. *Russ. J. Inorg. Chem.*, 2022, **67** (6), P. 799–809.
[58] Ostroushko A.A., Zhulanova T.Yu., Kudukov E.V., Gagarin I.D., Russkikh O.V. Lanthanum manganite nanopowders synthesis via combustion reactions under the influence of electromagnetic field. *Phys. Chem. Aspect. Stud. Clust. Nanostr. Nanomater.*, 2022, (14), P. 820–828.
[59] Ostroushko A.A., Russkikh O.V., Maksimchuk T.Yu. Charge generation during the synthesis of doped lanthanum manganites via combustion of organo-inorganic precursors. *Ceram. Int.*, 2021, **47** (15), P. 21905–21914.
[60] Filonova E.A., Russkikh O.V., Skutina L.S., Vylkov A.I., Maksimchuk T.Yu., Ostroushko A.A. $Sr_2Ni_{0.7}Mg_{0.3}MoO_{6-\delta}$: Correlation between synthesis conditions and functional properties as anode material for intermediate-temperature SOFCs. *Int. J. Hydrog.*, 2021, **46** (72), P. 35910–35922.
[61] Ostroushko A.A., Sennikov M.Yu. Thermochemical charge generation in polymer-salt films. *Russ. J. Inorg. Chem.*, 2005, **50** (6), P. 933–936.
[62] Ostroushko A.A., Sennikov M.Yu. Thermochemical charge generation in polymer-salt films as a function of temperature. *Russ. J. Inorg. Chem.*, 2008, **53** (8), P. 1172–1175.
[63] Filonova E.A., Russkikh O.V., Skutina L.S., Kochetova N.A., Korona D.V., Ostroushko A.A. Influence of synthesis conditions on phase formation and functional properties of prospective anode material $Sr_2Ni_{0.75}Mg_{0.25}MoO_{6-\delta}$. *J. Alloys Compd.*, 2018, **748**, P. 671–678.
[64] Martirosyan K.S., Filimonov I.A., Luss D. Electric-field generation by gas-solid combustion. *AIChE J.*, 2004, **50** (1), P. 241–248.
[65] Markov A.A., Filimonov I.A., Poletaev A.V., Vadchenko S.G., Martirosyan K.S. Generation of charge carriers during combustion synthesis of sulfides. *Int. J. Self-Propag. High-Temp. Synth.*, 2013, **22** (2), P. 69–76.
[66] Martirosyan K.S., Setoodeh M., Luss D. Electric-field generated by the combustion of titanium in nitrogen. *J. Appl. Phys.*, 2005, **98** (5), 054901.
[67] Setoodeh M., Martirosyan K.S., Luss D. Electrical pulse formation during high temperature reaction between Ni and Al. *J. Appl. Phys.*, 2006, **99** (8), 084901.
[68] Filimonov I., Luss D. Formation of electric potential during the oxidation of a metal particle. *AIChE J.*, 2004, **50** (9), P. 2287–2296.
[69] Filimonov I., Kidin N. Formation of charged defects during the nitridation of a metal particle. *Proc. Combust. Inst.*, 2007, **31** (2), P. 1991–1999.
[70] Kuznetsov M.V., Belousova O.V., Morozov Yu.G., Schipakin S.Yu. Electromotive force of combustion in the periodical table. *ISJAEE*, 2014, **20** (160), 38.
[71] Martirosyan K.S., Filimonov I.A., Nersesyan M.D., Luss D. Electric Field Formation during Combustion of Single Metal Particles. *J. Electrochem. Soc.*, 2003, **150** (5), P. 9–16.
[72] Gubin S.P., Koksharov Y.A., Khomutov G.B., Yurkov G.Y. Magnetic nanoparticles: preparation, structure and properties. *Russ. Chem. Rev.*, 2005, **74** (6), P. 489–520.
[73] Zhang N., Yang W., Ding W., Xing D., Du Y. Grain size-dependent magnetism in fine particle perovskite, $La_{1-x}Sr_xMnO_z$. *Solid State Communications*, 1999, **109** (8), P. 537–542.
[74] Walker D.A., Kowalczyk B., De La Cruz M.O., Grzybowski B.A. Electrostatics at the nanoscale. *Nanoscale*, 2011, **3** (4), P. 1316–1344.
[75] Genz U., Aguanno B.D., Mewis J. Structure of Sterically Stabilized Colloids. *Langmuir*, 1994, **10**, P. 2206–2212.
[76] Shankar A., Safronov A.P., Mikhnevich E.A., Beketov I.V., Kurlyandskaya G.V. Ferrogels based on entrapped metallic iron nanoparticles in a polyacrylamide network: extended Derjaguin–Landau–Verwey–Overbeek consideration, interfacial interactions and magnetodeformation. *Soft Matter*, 2017, **13** (18), P. 3359–3372.
[77] Skomski R. Nanomagnetics. *J. Phys.: Condens. Matter*, 2003, **15** (20), R841–R896.
[78] Ivanov A.O., Zubarev A. Chain Formation and Phase Separation in Ferrofluids: The Influence on Viscous Properties. *Materials*, 2020, **13** (18), 3956.
[79] Mikhnevich E.A., Chebotkova P.D., Safronov A.P. Synthesis and Study of Mechanical Properties of Polyelectrolyte Ferrogels Based on Strontium Ferrite Particles. *Inorg. Mater. Appl. Res.*, 2020, **11** (4), P. 855–860.
[80] Sanchez-Dominguez Ed. M., Rodriguez-Abreu C. *Nanocolloids: a meeting point for scientists and technologists*. Elsevier, Amsterdam, 2016, 514 p.
[81] Lim J.K., Majetich S.A., Tilton R.D. Stabilization of Superparamagnetic Iron Oxide Core-Gold Shell Nanoparticles in High Ionic Strength Media. *Langmuir*, 2009, **25** (23), P. 13384–13393.
[82] Almjasheva O.V., Popkov V.I., Proskurina O.V., Gusarov V.V. Phase formation under conditions of self-organization of particle growth restrictions in the reaction system. *Nanosystems: Phys. Chem. Math.*, 2022, **13** (2), P. 164–180.
[83] Almjasheva O.V., Lomanova N.A., Popkov V.I., Proskurina O.V., Tugova E.A., Gusarov V.V. The minimum size of oxide nanocrystals: phenomenological thermodynamic vs crystal-chemical approaches. *Nanosystems: Phys. Chem. Math.*, 2019, **10** (4), P. 428–437.
[84] Kantorovich S.S., Ivanov A.O., Rovigatti L., Tavares J.M., Sciortino F. Temperature-induced structural transitions in self-assembling magnetic nanocolloids. *Phys. Chem. Chem. Phys.*, 2015, **17** (25), P. 16601–16608.
[85] Urusova N., Kumar M.R., Semkin M., Filonova E., Kratochvilova M., Neznakhin D., et al. Crystal structure and magnetic properties of $Sr_2Ni_{1-x}Mg_xMoO_6$ ($x = 0$, 0.25, 0.5, and 0.75) polycrystals. *Solid State Sci.*, 2020, **99**, 106008.
[86] Ostroushko A.A. *Physico-chemical bases of obtaining solid-phase materials for electronic engineering and catalysis: students guide*. UrFU, Ekaterinburg, 2011, 160 p. (in Russian).

Submitted 27 July 2023; revised 6 October 2023; accepted 8 October 2023

Information about the authors:

Alexander A. Ostroushko – Ural Federal University Scientific Research Institute of Physics and Applied Mathematics, Ekaterinburg 620002, Russia; ORCID 0000-0003-0206-5513; alexander.ostroushko@urfu.ru

Iliya D. Gagarin – Ural Federal University Scientific Research Institute of Physics and Applied Mathematics, Ekaterinburg 620002, Russia; ORCID 0000-0002-8545-927X; ilya.gagarin@urfu.ru

Egor V. Kudyukov – Ural Federal University Scientific Research Institute of Physics and Applied Mathematics, Ekaterinburg 620002, Russia; ORCID 0000-0002-4382-7695; e.v.kudyukov@urfu.ru

Tatiana Yu. Zhulanova – Ural Federal University Scientific Research Institute of Physics and Applied Mathematics, Ekaterinburg 620002, Russia; ORCID 0000-0002-8009-4398; tatiana.maksimchuk@urfu.ru

Anastasya E. Permyakova – Ural Federal University Scientific Research Institute of Physics and Applied Mathematics, Ekaterinburg 620002, Russia; ORCID 0009-0004-3194-4626; nastia2605permiakova@yandex.ru

Olga V. Russkikh – Ural Federal University Scientific Research Institute of Physics and Applied Mathematics, Ekaterinburg 620002, Russia; ORCID 0000-0001-5923-095X; o.v.russkikh@urfu.ru

Conflict of interest: the authors declare no conflict of interest.